This article has been accepted for publication in a future issue of this journal, but has not been fully edited. Content may change prior to final publication. Citation information: DOI 10.1109/TSTE.2018.2878230, IEEE Transactions on Sustainable Energy

Capacity Planning of Energy Hub in Multi-carrier Energy Networks: A Data-driven Robust Stochastic Programming Approach

Yang Cao, *Student Member, IEEE,* Wei Wei, *Senior Member, IEEE*, Jianhui Wang, *Senior Member, IEEE,* Shengwei Mei, *Fellow, IEEE,* Miadreza Shafie-khah, *Senior Member, IEEE,* João P. S. Catalão, *Senior Member, IEEE*

***Abstract*—Cascaded utilization of natural gas, electric power, and heat could leverage synergetic effects among these energy resources, precipitating the advent of integrated energy systems. In such infrastructures, energy hub is an interface among different energy systems, playing the role of energy production, conversion and storage. The capacity of energy hub largely determines how tightly these energy systems are coupled and how flexibly the whole system would behave. This paper proposes a data-driven two-stage robust stochastic programming model for energy hub capacity planning with distributional robustness guarantee. Renewable generation and load uncertainties are modelled by a family of ambiguous probability distributions near an empirical distribution in the sense of Kullback-Leibler (KL) divergence measure. The objective is to minimize the sum of the construction cost and the expected life-cycle operating cost under the worst-case distribution restricted in the ambiguity set. Network energy flow in normal operating conditions is considered; demand supply reliability in extreme conditions is taken into account via robust chance constraints. Through duality theory and sampling average approximation, the proposed model is transformed into an equivalent convex program with a nonlinear objective and linear constraints, and is solved by an outer-approximation algorithm which entails solving only linear program. Case studies demonstrate the effectiveness of the proposed model and method.**

***Index Terms*—capacity planning, data-driven optimization, energy hub, multi-carrier energy system, uncertainty**

NOMENCLATURE

A. Abbreviations

CHP	Combined heat and power.
COP	Coefficient of performance.
DC	Direct current.
DHN	District heating network.
DR-SP	Data-driven robust stochastic programming.
ESU	Electricity storage unit.
HP	Heat pump.
KL	Kullback-Leibler.
LP	Linear program.
MILP	Mixed-integer linear program.
MINLP	Mixed-integer nonlinear program.
PDF	Probability density function.
PDN	Power distribution network.
OA	Outer approximation.
RO	Robust optimization.
SP	Stochastic programming.
SAA	Sampling average approximation.
TSU	Thermal storage unit.

B. Sets

$S_j^{B,d}$	Set of downstream buses connecting to bus j.
$S_i^{P,s}$	Set of pipelines starting at node i.
$S_i^{P,e}$	Set of pipelines ending at node i.

C. Parameters

c_p	Specific heat capacity of water.
COP_i	COP of heat pump.
$h_{i,t}^L$	Heat loads.
I^s	Per unit construction cost of component s.
L_b	Length of pipeline b in the DHN.
$\dot{m}_{i,t}^S/\dot{m}_{i,t}^L$	Mass flow rate of heat source/load.
$\dot{m}_{b,t}$	Mass flow rate in pipeline b.
$p_{j,t}^d/q_{j,t}^d$	Active/reactive power demands.
r_{ij}/x_{ij}	Line resistance/reactance.
T_t^a	Ambient temperature in period t.
V_0	Voltage magnitude at the slack bus.
$\eta_{i,c}^E/\eta_{i,d}^E$	Charge/discharge efficiency of the ESU.
$\eta_{i,c}^T/\eta_{i,d}^T$	Charge/discharge efficiency of the TSU.
η_i^{gp}/η_i^{gh}	Gas to power/heat efficiency of CHP unit.
λ_b	Heat transfer coefficient of pipelines.
μ_i^E	Self-discharge rate of ESU.
μ_i^T	Thermal dissipation rate of TSU.
ω_g	Price of natural gas.

The work of Y. Cao, W. Wei and S. Mei was supported in part by the National Natural Science Foundation of China (51807101, U1766203, 51621065). M. Shafie-khah and J. P. S. Catalão acknowledge the support by FEDER funds through COMPETE 2020 and by Portuguese funds through FCT, under Projects SAICT-PAC/0004/2015 - POCI-01-0145-FEDER-016434, POCI-01-0145-FEDER-006961, UID/EEA/50014/2013, UID/CEC/50021/2013, UID/EMS/00151/2013, and 02/SAICT/2017 - POCI-01-0145-FEDER-029803. *Corresponding author: S. Mei.*

Y. Cao, W. Wei, S. Mei, are with the State Key Laboratory of Power Systems, Department of Electrical Engineering, Tsinghua University, Beijing, 100084, China (e-mails: cao-y17@mails.tsinghua.edu.cn, wei-wei04@mails.tsinghua.edu.cn, meishengwei@tsinghua.edu.cn).

J. Wang is with the Department of Electrical Engineering at Southern Methodist University, Dallas, TX 75205 USA (e-mail: jianhui@smu.edu).

M. Shafie-khah is with INESC TEC, Porto 4200-465, Portugal (e-mail: miadreza@gmail.com).

J. P. S. Catalão is with INESC TEC and the Faculty of Engineering of the University of Porto, Porto 4200-465, Portugal, also with C-MAST, University of Beira Interior, Covilhã 6201-001, Portugal, and also with INESC-ID, Instituto Superior Técnico, University of Lisbon, Lisbon 1049-001, Portugal (e-mail: catalao@ubi.pt).

This article has been accepted for publication in a future issue of this journal, but has not been fully edited. Content may change prior to final publication. Citation information: DOI 10.1109/TSTE.2018.2878230, IEEE Transactions on Sustainable Energy

D. Decision Variables

C^s	Capacity of component s in energy hub.
$g_{i,t}^{in}$	Gas input of energy hub.
$h_{i,t}^{out}$	Heat output of energy hub.
$h_{i,t}^{c}/h_{i,t}^{d}$	Charge/discharge rate of TSU.
$h_{i,t}^{HP}$	Heat output of heat pump.
$P_{ij,t}/Q_{ij,t}$	Active/reactive line power flow.
$p_{i,t}^{c}/p_{i,t}^{d}$	Charge/discharge rate of ESU.
$p_{i,t}^{in}/p_{i,t}^{out}$	Electric power input/output of energy hub.
$p_{i,t}^{TU}/p_{i,t}^{w}$	Output of local generator/wind farm.
$p_{i,t}^{CHP}/h_{i,t}^{CHP}$	Electric/thermal power output of CHP unit.
$V_{j,t}$	Voltage magnitude at bus j.
$W_{i,t}^{E}$	Electrical energy stored in ESU.
$W_{i,t}^{T}$	Thermal energy stored in TSU.
$\tau_{b,t}^{i}/\tau_{b,t}^{o}$	Temperature at inlet/outlet of pipeline b.
$\tau_{i,t}^{S}/\tau_{i,t}^{R}$	Temperature of heat source or load at supply/ return side.
$\tau_{i,t}^{n}$	Mixture temperature at node i.

I. Introduction

THE excessive consumption of coals has created serious air pollution problems in modern society. The Shale Rock Revolution makes natural gas a promising clean fuel in the future. Meanwhile, the proliferation of renewable energy resources such as wind and solar generation greatly reduces the carbon dioxide emission from the electricity sector. Nevertheless, the output of wind farms and photovoltaic panels is volatile, requiring sufficient backup capacity and flexible resources to compensate the real-time imbalance, which has brought great challenges to power system operation. Gas-fired unit is able to respond to the fast change of renewable output; heating system has large thermal inertial and could serve as energy storage [1], [2]. Furthermore, combined dispatch of natural gas, heat and power generation enjoys higher efficiency than separated operation due to the cascade utilization of various energies [3], [4]. In a word, considering the integration of multi-carrier energy could improve overall energy efficiency through cascaded usage of energy, and enhance system flexibility by leveraging the fast-response and storage capabilities of gas and heating systems. On this account, energy system integration has become a prevalent trend in recent years, precipitating the advent of multi-carrier energy systems [5], [6]. In such integrated infrastructures, the connection (interface) facility is the so-called energy hub [7], [8], which plays the role of energy production, conversion and storage.

Operation of multi-carrier energy systems with energy hubs has been the research focus during the past few years. Residential-level energy hub refers to those appearing at the demand side and directly supplying home appliance without considering network constraints since their capacity is small and a single hub has tiny effect on the distribution system. The operation of such energy hubs are formulated as a mixed-integer linear program (MILP) in [9] and a mixed-integer nonlinear program (MINLP) in [10]. Operation and flexibility of energy hub in combined heating, cooling and power generation systems are studied in [11] through MINLP based approach. Reference [12] investigates the operation of energy hub in a smart building comprised of electric vehicles, combined heat and power (CHP) unit, solar panels, and electrical storage system. Distribution-level energy hub categories those connecting to natural gas, power, and heat distribution systems and acting as a prosumer. Because their operation could affect system energy flows, network models have to be incorporated. Along this line of research, the multi-carrier optimal energy flow is discussed in [13]. A decomposition method and a multi-agent genetic algorithm is applied to solve the problem. An MILP model is suggested in [14] to solve the optimal energy flow problem based on piecewise linear approximation of non-convex natural gas flow constraints. A decomposition approach is developed in [15] to solve the optimal energy flow problem with a holomorphic embedding method to calculate power flow solution of the electricity sub-network.

In above system operation studies, capacities of generation equipment, energy conversion facilities, and storage units in the energy hub are given, and largely determine how tightly individual systems are coupled with each other and how flexibly the whole system would behave. Energy hub capacity planning is another focus in the research field. For residential-level energy hubs, a graphic theory based configuration modeling method is set forth in [16], and the optimal configuration planning problem comes down to an MILP. A two-stage MILP model for energy hub configuration is developed in [17], in which both equipment selection and connection topology are optimized. As for the planning of distribution-level energy hub connecting multi-carrier energy systems, reference [18] investigates the optimal expansion planning for energy hub in the interdependent natural gas and electricity networks considering reliability, energy efficiency and carbon emission. This problem is also studied in [19] by considering cooling demands additionally. In [20], the planning strategies of energy hub, power grid and natural gas system are jointly optimized, ameliorating energy supply economy and system reliability.

Most of aforementioned studies rely on a deterministic optimization paradigm. However, uncertain factors are ubiquitous in the multi-carrier energy system, such as the volatility of renewable generation and fluctuations of load demands. To cope with uncertainty during the planning stage, a scenario based stochastic programming (SP) approach is proposed in [21] to address the optimal planning of energy hub with uncertain wind power, electricity price and demand. The SP approach is employed in [22] to design a wind integrated energy hub, where both economic cost and reliability indices are taken into account. In [23], an SP model is introduced to address the demand response programs considering the uncertainty of customers' decisions in the multi-carrier energy systems. Computational issue may arise in SP approaches because a large number of scenarios are required to reflect the random nature more accurately, leading to problems with very large sizes. Benders decomposition algorithm is used in [24] to solve SP models of energy hub planning problems. Robust optimization (RO) is another useful tool for decision making under uncertainty, which protects the system against the worst-case scenario, but tends to be somehow conservative due to the low probability of extreme events. RO is applied in energy hub scheduling problem with unknown parameters [25], as well as

This article has been accepted for publication in a future issue of this journal, but has not been fully edited. Content may change prior to final publication. Citation information: DOI 10.1109/TSTE.2018.2878230, IEEE Transactions on Sustainable Energy

operation and planning of multi-carrier energy systems [26]–[28], but rarely seen in energy hub capacity planning problems, to the best of our knowledge.

SP and RO have their own advantages and drawbacks. The former one needs the exact probability distribution of uncertain factors and offers an optimal solution in the sense of statistics. However, the exact distribution is usually difficult to acquire due to the lack of enough data; furthermore, despite that an approximated distribution can be procured, the optimal solution to an SP model could have poor statistical performances if the actual distribution is not identical to the designated one [29]. RO neglects the dispersion effect of uncertainty and copes with the worst-case scenario in a pre-defined uncertainty set, and the solution performance is insensitive to the change of uncertain parameter as long as it does not step outside the uncertainty set. Nevertheless, as the worst-case scenario rarely happens in reality, the robust strategy could be conservative thus suboptimal in practice. A method which combines the advantages of SP and RO is the distributionally RO [30], [31], which is also called data-driven robust SP (DR-SP) [32]. This approach minimizes the expected cost under the worst-case probability distribution within a family of candidate distributions rather than an exact distribution or a specific scenario. The optimal strategy is less conservative than traditional RO method and more robust against perturbation in the PDF of uncertain data than traditional SP model. Due to the difference in uncertainty models, the solution algorithms of SP, RO and DR-SP also differ a lot.

In this paper, a two-stage DR-SP model is set forth for determining optimal facility sizes in a distribution-level energy hub. The contributions are summarized as follows.

1) We propose a DR-SP approach to address energy hub capacity planning problem in multi-carrier energy networks. Renewable generation and load uncertainties are modelled by ambiguous probability density functions (PDFs) around an empirical PDF constructed from moderate historical data. The distance between two PDFs is quantified by Kullback-Leibler (KL) divergence measure. The objective function minimizes the sum of investment cost and expected operating cost across the service period under the worst-case distribution restricted in the ambiguity set. Supply reliability in extreme conditions are modeled by robust chance constraints. Compared to conventional SP and RO approaches, the proposed method requires moderate information on uncertainty, and provides robust planning strategies with reasonable conservatism level, which could be adjusted by changing the KL-divergence parameter in the ambiguity set.

2) We develop tractable reformulations for the proposed model which is originally nonconvex and nonlinear, due to the min-max-min objective function and robust chance constraints. The constraints are linearized via convex approximation and sampling average approximation (SAA). The objective function is transformed to a purely minimization one via dual theory. We reveal its convexity and develop an outer-approximation (OA) algorithm in order to efficiently solve the whole problem using LP solvers. Case studies validate the good performance of the proposed method.

The rest of the paper is organized as follows. Mathematical formulation of the DR-SP model for energy hub capacity planning is introduced in Section II; The solution strategy is developed in Section III; Case studies are carried out in Section IV to demonstrate the effectiveness of the proposed model and algorithm; Finally, conclusion is summarized in Section V.

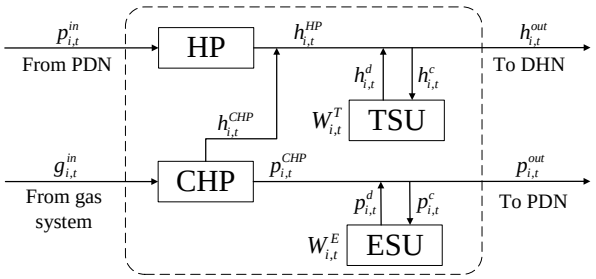

Fig. 1. Structure of energy hub.

II. Mathematical Formulation

A. Energy Hub Model

The topology and energy flow variables of energy hub are shown in Fig. 1. The inputs are electricity and natural gas; the outputs are electricity and heat. The energy hub consists of CHP unit, heat pump (HP), electricity storage unit (ESU) and thermal storage unit (TSU). Different from residential energy hubs whose output connects to end users, both sides of the hub in Fig. 1 connect to energy systems. Operating constraints and energy flows in the energy hub can be described as follows:

$$p_{i,t}^{out} = p_{i,t}^{CHP} + p_{i,t}^{d} - p_{i,t}^{c} \tag{1a}$$

$$h_{i,t}^{out} = h_{i,t}^{CHP} + h_{i,t}^{HP} + h_{i,t}^{d} - h_{i,t}^{c} \tag{1b}$$

$$g_{i,t}^{in} = p_{i,t}^{CHP}/\eta_i^{gp} + h_{i,t}^{CHP}/\eta_i^{gh} \tag{1c}$$

$$h_{i,t}^{HP} = \mathrm{COP}_i \cdot p_{i,t}^{in} \tag{1d}$$

$$W_{i,t+1}^{E} = W_{i,t}^{E}(1-\mu_i^{E}) + (p_{i,t}^{c}\eta_{i,c}^{E} - p_{i,t}^{d}/\eta_{i,d}^{E})\Delta t \tag{1e}$$

$$W_{i,t+1}^{T} = W_{i,t}^{T}(1-\mu_i^{T}) + (h_{i,t}^{c}\eta_{i,c}^{T} - h_{i,t}^{d}/\eta_{i,d}^{T})\Delta t \tag{1f}$$

where equalities (1a) and (1b) are electric and thermal power balancing conditions; equations (1c) and (1d) stipulate the input-output relations of CHP unit and HP. Constraints (1e) and (1f) describe charging dynamics of ESU and TSU. Complementarity of charging and discharging is naturally met and thus relaxed in (1), because simultaneous charging and discharging is not the optimal strategy owing to dissipativity. Detailed analysis can be found in [33]. Strict complementarity can be imposed in model (1) via binary variables without jeopardizing the solution method discussed later.

B. Network Models

The power distribution network (PDN) is radial in topology, and the power flow in PDN can be established recursively from the linearized branch flow model developed in [34].

$$p_{j,t} + P_{ij,t} = \sum\nolimits_{k \in S_j^{B,d}} P_{jk,t} + p_{j,t}^{d} \tag{2a}$$

This article has been accepted for publication in a future issue of this journal, but has not been fully edited. Content may change prior to final publication. Citation information: DOI 10.1109/TSTE.2018.2878230, IEEE Transactions on Sustainable Energy

$$q_{j,t} + Q_{ij,t} = \sum\nolimits_{k \in S_j^{B,d}} Q_{jk,t} + q_{j,t}^d \tag{2b}$$

$$V_{j,t} = V_{i,t} - (r_{ij} P_{ij,t} + x_{ij} Q_{ij,t})/V_0 \tag{2c}$$

where equalities (2a) and (2b) represent active and reactive power balancing conditions, $p_{j,t}$ denotes the total active power injection at bus j, including the active output from local generators $p_{j,t}^{TU}$, wind farms $p_{j,t}^{w}$, and the energy hub $p_{j,t}^{out}$. Equality (2c) stands for the forward voltage drop along a distribution line. Model (2) neglects network losses; nevertheless, reactive power and bus voltage are considered, so it is more appropriate in distribution systems than the well-known DC power flow model which neglects reactive power and assumes constant bus voltage magnitudes.

A district heating network (DHN) consists of symmetric supply and return pipelines. At each source (load) node, heat is injected into (withdrawn from) the network via a heat exchanger between the supply side and the return side. The physical DHN model is subject to hydraulic conditions and thermal conditions [35]. In this paper, the constant-flow variable temperature mode is adopted, in which mass flow rates $\dot{m}$ in hydraulic conditions are set to constant values. The thermal flow model of DHN reads as follows.

$$h_{i,t}^S = c_p \dot{m}_{i,t}^S (\tau_{i,t}^S - \tau_{i,t}^R) \tag{3a}$$

$$h_{i,t}^L = c_p \dot{m}_{i,t}^L (\tau_{i,t}^S - \tau_{i,t}^R) \tag{3b}$$

$$\tau_{b,t}^o = (\tau_{b,t}^i - T_t^a) e^{-\frac{\lambda_b L_b}{c_p \dot{m}_{b,t}}} + T_t^a \tag{3c}$$

$$\sum\nolimits_{b \in S_i^{P,e}} (\tau_{b,t}^o \dot{m}_{b,t}) = \tau_{i,t}^n \sum\nolimits_{b \in S_i^{P,e}} \dot{m}_{b,t} \tag{3d}$$

$$\tau_{b,t}^i = \tau_{i,t}^n \quad \forall b \in S_i^{P,s} \tag{3e}$$

where equalities (3a) and (3b) represent thermal energy exchange at heat source and heat load nodes. Equality (3c) describes the temperature drops along the supply/return pipelines. Equality (3d) depicts the mixture fluid temperature at confluence nodes. Equality (3e) stipulates the temperature of mass flows leaving a confluence node. For more details about the DHN, please refer to [35].

Gas flows in a pipeline network are governed by partial differential equations [36], and gas-electricity coupling usually appears at transmission level. This paper focuses on heat-power integration at distribution level: the interdependent PDN and DHN in a city, as heat cannot be economically delivered for very long distance. Therefore, natural gas transportation network model in an upstream level is neglected. Transients in a gas distribution network are usually much faster. The main operating limit for an energy hub is the maximum gas deliver rate, which can be roughly approximated by imposing time-varying upper bounds on the natural gas inflows.

C. Deterministic Model

In the deterministic formulation, renewable output and load demands are known exactly. In the first stage, capacities of energy hub components are determined; in the second stage, operating constraints in three typical days (sampled from spring/autumn, summer, and winter) are considered. The objective function is to minimize the sum of construction cost and life-cycle operation cost. We make the following assumptions in the planning problem:

1) Energy hub planning is guided by a government agency. The objective is to minimize the investment cost of the hub and the total operation cost of the integrated energy system during a period of 10 years. Because we consider a distribution-level energy hub, whose operation cost is comparable to that of the system, the two costs can be added together for minimization.
2) The connection topology of the energy hub is fixed. The candidate components for investment include CHP unit, HP, ESU and TSU. Electric boilers and different types of battery arrays can be easily included. For the ease of exposition, we just select one typical facility for each functionality when establishing the model. The operation cost consists of fuel expenditures of local generators in the PDN and the CHP unit in the energy hub.
3) The cost of heat pump is neglected for two reasons: First, it consumes electricity whose production cost has already been counted; Second, the cost of heat pump, if exists, is paid by the energy hub to the PDN, i.e., a domestic financial issue inside the integrated energy system, so does not appear in the objective function.

Conceptually, the deterministic energy hub planning problem can be written as follows

$$\begin{aligned} \min \quad & f_C + N_d \cdot f_O \\ \text{s.t.} \quad & \text{Cons-PF},\ \text{Cons-TF} \\ & \text{Cons-EH},\ \text{Cons-BD} \end{aligned} \tag{4}$$

where Cons-PF stands for the linearized branch flow equations (2a)-(2c); Cons-TF is the abbreviation for thermal flow constraints (3a)-(3e); Cons-EH encapsulates energy hub operation conditions in (1); Cons-BD collects all lower and upper bound constraints of decision variables. The construction cost is given by

$$f_C = I^{CHP} C^{CHP} + I^{HP} C^{HP} + I^E C^E + I^T C^T \tag{5}$$

which includes investment costs of CHP unit, heat pumps, ESU and TSU in the energy hub. The daily operation cost function is defined as

$$f_O = \sum_t \left(\sum_i \omega_g g_{i,t}^{in} + \sum_j F(p_{j,t}^{TU}) \right) \tag{6}$$

which consists of fuel costs of CHP units and local generators. The convex quadratic function $F(p_j^{TU})$ can be approximated by a piecewise linear function using well-known methods, such as that in [37], so we can assume that the objective function is linear without loss of generality. N_d is the number of services days, which is equal to 3650 in this paper. For notation conciseness, a typical day is selected to explain the model; in implementation, we incorporate three typical days in spring/autumn, summer, and winter with weights 0.5, 0.25 and 0.25 to calculate the daily operation cost f_O. Here we do not consider demand growth and net present value of operation cost, because a 10-year planning horizon is

This article has been accepted for publication in a future issue of this journal, but has not been fully edited. Content may change prior to final publication. Citation information: DOI 10.1109/TSTE.2018.2878230, IEEE Transactions on Sustainable Energy

relatively moderate. Nevertheless, such factors can be easily incorporated by modifying some parameters.

The bounds of energy hub operating variables depend on capacities of CHP unit C^{CHP}, heat pump C^{HP}, ESU C^E and TSU C^T. Their relations are

$$(p_{i,t}^{CHP}/\eta_i^{gp} + h_{i,t}^{CHP}/\eta_i^{gh}) \le C^{CHP} \tag{7a}$$

$$p_{i,t}^{CHP}/\eta_i^{gp} \ge R_g^p C^{CHP}, h_{i,t}^{CHP}/\eta_i^{gh} \le R_g^h C^{CHP} \tag{7b}$$

$$h_{i,t}^{HP} \le C^{HP} \tag{7c}$$

$$W_{i,t}^E \le C^E, p_{i,t}^d \le R_d^E C^E, p_{i,t}^c \le R_c^E C^E \tag{7d}$$

$$W_{i,t}^T \le C^T, h_{i,t}^d \le R_d^T C^T, h_{i,t}^c \le R_c^T C^T \tag{7e}$$

which are included in Cons-BD. The former two equalities denote the polyhedral operation region of CHP unit, including the maximum fuel import rate in (7a), as well as minimum electric output and maximum thermal output in (7b), where R_g^h and R_g^p are constants; (7c) reflects HP capacity; Equalities (7d) and (7e) limit the charging/discharging rates of storage units depending on their capacities, where R_d^E, R_c^E, R_d^T and R_c^T are constants.

Let vector $\boldsymbol{x}$ represent the first-stage decision variables, i.e., facility capacities C^{CHP}, C^{HP}, C^E and C^T; vector $\boldsymbol{\xi}$ denotes the uncertain parameters including the output of wind farms $p_{j,t}^w$ and system loads $p_{j,t}^d$ and $h_{i,t}^L$; vector $\boldsymbol{y}$ contains the second-stage decision variables, including those in the power flow model and the thermal flow model. With notations defined above, the deterministic model for energy hub planning is an LP and can be expressed via a compact matrix form as follows

$$\begin{aligned} \min\ & \boldsymbol{c}^T\boldsymbol{x} + Q(\boldsymbol{x}, \boldsymbol{\xi}) \\ \text{s.t. } & \boldsymbol{x} \in X \end{aligned} \tag{8}$$

where $X = \{\boldsymbol{x} | \boldsymbol{0} \le \boldsymbol{x} \le \boldsymbol{x^u}\}$ is the feasible set of first-stage decisions; the first term $\boldsymbol{c}^T\boldsymbol{x}$ in the objective function corresponds to the construction cost f_C in (5); the second term $Q(\boldsymbol{x}, \boldsymbol{\xi})$ is the optimal operating cost associated with parameter $\boldsymbol{\xi}$ under a given $\boldsymbol{x}$, which can be expressed by

$$\begin{aligned} Q(\boldsymbol{x}, \boldsymbol{\xi}) = \min_{\boldsymbol{y}}\ & \boldsymbol{p}^T\boldsymbol{y} \\ \text{s.t. } & \boldsymbol{A}\boldsymbol{x} + \boldsymbol{B}\boldsymbol{y} + \boldsymbol{C}\boldsymbol{\xi} + \boldsymbol{d} \le 0 \end{aligned} \tag{9}$$

where the objective function corresponds to the operation cost in (6). Constraints include those in Cons-PF, Cons-TF, Cons-EH, and Cons-BD, except for those in X.

Without uncertainty, problem (8) is an LP and can be easily solved. To explain why the planning problem is posed in a two-stage form, let us see how the uncertainty is dealt with. To actively consider the uncertain nature of parameter $\boldsymbol{\xi}$, SP and RO models can be set up based on the deterministic formulation (8). Suppose we have a set of representative samples $\boldsymbol{\xi}^1$, $\boldsymbol{\xi}^2$, $\cdots$, $\boldsymbol{\xi}^n$. For the scenario based SP, if we know the probabilities π_1, π_2, $\cdots$, π_n with respect to each sample, then the SP model can be set up by

$$\begin{aligned} \min\ & \boldsymbol{c}^T\boldsymbol{x} + \sum_n \pi_n \boldsymbol{p}^T\boldsymbol{y}^n \\ \text{s.t. } & \boldsymbol{x} \in X,\ \boldsymbol{A}\boldsymbol{x} + \boldsymbol{B}\boldsymbol{y}^n + \boldsymbol{C}\boldsymbol{\xi}^n + \boldsymbol{d} \le 0,\ \forall n \end{aligned} \tag{10}$$

Otherwise, if no information on the probabilities is available, we can resort to the following RO model

$$\begin{aligned} \min_{\boldsymbol{x}}\ & \boldsymbol{c}^T\boldsymbol{x} + \max_{\boldsymbol{\xi}^n} \left\{ \min_{\boldsymbol{y}^n} \boldsymbol{p}^T\boldsymbol{y}^n \right\} \\ \text{s.t. } & \boldsymbol{x} \in X,\ \boldsymbol{A}\boldsymbol{x} + \boldsymbol{B}\boldsymbol{y}^n + \boldsymbol{C}\boldsymbol{\xi}^n + \boldsymbol{d} \le 0,\ \forall n \end{aligned} \tag{11}$$

From (10) and (11) we can observe:

1) The second-stage decision $\boldsymbol{y}^n$ depends on the value of first-stage decision $\boldsymbol{x}$ and uncertain data $\boldsymbol{\xi}^n$. This refers to the fact that once the capacity planning strategies of energy hub are deployed in the first-stage, they cannot change any more during the operation periods. The second stage simulates system daily operation after the uncertain data (e.g. renewable generation and load demand) can be predicted accurately. This means that the output of each unit could respond to the actual value of uncertain data to minimize the operation cost. In this way, planning and operation are integrated in a holistic model through taking detailed operation constraints and data uncertainty into account in the planning stage.
2) SP and RO models share the same constraints; they are different in the objective function: the former incorporates an expected cost in the second stage, and the latter considers the worst-case outcome. Clearly, SP requires more information on the uncertainty. In practice, we may not have exact values of π_n, but can still infer some useful information from finite historical data available at hand, such as an empirical distribution, and how close the true one is distant to the empirical one. But if we use RO model (11), we naturally abandon all the distribution information, and may get over-conservative planning strategies. Above dilemma calls for new methodology that utilizes ambiguous dispersion information and remains computationally tractable.

D. Modelling the Uncertainty

1) Determining a reference distribution P_0. The most widely used empirical distribution is the histogram. For example, we have totally M samples to fit in N bins, and there are M_1, M_2, $\cdots$, M_N samples in each bin. Then the representative scenario in each bin is the expectation of $\boldsymbol{\xi}$ in there, and the corresponding probability is $\pi_i = M_i/M$, $i = 1, \cdots, N$, and the discrete density function of P_0 is $\{\pi_1, \cdots, \pi_N\}$. Otherwise, we may assume that $\boldsymbol{\xi}$ follows some certain distribution, say the Gaussian distribution, and calibrate the parameters in the PDF via curve fitting methods [38]. Because we will consider a family of PDFs around P_0, the requirement on an accurate distribution can be relaxed.

2) Constructing the ambiguity set. We consider all possible probability distributions that are close enough to P_0, or more exactly, all elements in the following set

$$W = \{P | D_{KL}(P \parallel P_0) \le d_{KL}\} \tag{12}$$

where d_{KL} is a constant threshold which determines the size of the ambiguity set and reflects the confidence level, and the

This article has been accepted for publication in a future issue of this journal, but has not been fully edited. Content may change prior to final publication. Citation information: DOI 10.1109/TSTE.2018.2878230, IEEE Transactions on Sustainable Energy

distance measure

$$D_{KL}(P \parallel P_0) = \int_{\Omega} f(\xi) \log \frac{f(\xi)}{f_0(\xi)} \mathrm{d}\xi \tag{13}$$

is the KL-divergence from the density function $f_0(\xi)$ of P_0 to the density function $f(\xi)$ of P. For discrete distributions, the KL-divergence has the form of

$$D_{KL}(P \parallel P_0) = \sum_{n} \pi_n \log \frac{\pi_n}{\pi_n^0} \tag{14}$$

In either case, there are infinitely many PDFs in the ambiguity set W whenever $d_{KL} > 0$; otherwise, if $d_{KL} = 0$, W becomes a singleton, and the proposed formulation degenerates to a traditional SP model.

KL-divergence is established based on information theory [39], and is widely adopted to quantify the distance between two probability distributions in distributionally RO problems. Later we will see, using such a measure in the ambiguity set W will give rise to a convex equivalent program, which greatly facilitates solving the planning problem.

3) Selecting the confidence level d_{KL}. In practice, the decision marker can specify the value of d_{KL} according to the attitude towards risks. Nevertheless, a proper value can be obtained from probability theory. Intuitively, the more historical data we have, the closer the reference PDF $f_0(\xi)$ leaves from the true one, and the smaller d_{KL} should be set. As indicated in Theorem 3.1 in [40], it could be selected as:

$$d_{KL} = \frac{1}{2M} \chi^2_{N-1,\alpha^*} \tag{15}$$

where χ^2_{N-1,α^*} is the α^* upper quantile of a χ^2 distribution with $N-1$ degrees of freedom. Equation (15) ensures that W contains the true distribution with a probability of at least α^*.

E. Data-driven Robust SP Model

Based on the compact form (8) and the ambiguity set W defined in (12), the DR-SP model for energy hub planning could be cast as

$$\min \quad \boldsymbol{c}^T \boldsymbol{x} + \sup_{P \in W} E_P[Q(\boldsymbol{x}, \boldsymbol{\xi})] \tag{16a}$$

$$\text{s.t.} \quad \boldsymbol{x} \in X \tag{16b}$$

$$\inf_{P' \in W'} \Pr\{D_{loss}(\boldsymbol{\xi}) \le 0\} \ge 1 - \alpha \tag{16c}$$

where $E_P[Q(\boldsymbol{x}, \boldsymbol{\xi})]$ denotes the expectation of operation cost value function $Q(\boldsymbol{x}, \boldsymbol{\xi})$ when the uncertain parameter $\boldsymbol{\xi}$ follows distribution P. Constraint (16c) prescribes that in extreme days, all load must be served with a minimal probability of $1-\alpha$, or the probability of load shedding must be smaller than α. We call it a robust chance constraint because it considers the worst-case distribution. $D_{loss}(\boldsymbol{\xi})$ means the minimum unserved load in extreme days given the uncertain data $\boldsymbol{\xi}$, which is defined as

$$\begin{aligned} D_{loss}(\boldsymbol{\xi}) = \min \quad & g \\ \text{s.t.} \quad & \boldsymbol{A'x} + \boldsymbol{B'y} + \boldsymbol{C'\xi} + \boldsymbol{d'} \le 0 \\ & \textstyle\sum_{k \in S_j^{b,d}} P_{jk,t} + p^d_{i,t} - P_{ij,t} - p_{j,t} \le g \\ & c_p \dot{m}^L_{i,t} (\tau^S_{i,t} - \tau^R_{i,t}) - h^L_{i,t} \le g \end{aligned} \tag{17}$$

where coefficient matrices $\boldsymbol{A'}$, $\boldsymbol{B'}$, $\boldsymbol{C'}$, and $\boldsymbol{d'}$ correspond to $\boldsymbol{A}$, $\boldsymbol{B}$, $\boldsymbol{C}$, and $\boldsymbol{d}$ excluding nodal energy balancing conditions. The latter two inequalities are relaxed nodal energy balancing conditions, in which load shedding is quantified by a slack variable g, and $\boldsymbol{\xi}$ collects all uncertain parameters including $p^w_{j,t}$, $p^d_{j,t}$ and $h^L_{i,t}$. Please note that in (17) we do not restrict g to be non-negative, and a negative g will not impact planning or operating strategies, because it is only used for evaluating load shedding probability and will never be deployed for operation purpose.

The objective function (16a) accounts for the expectation $E_P[Q(\boldsymbol{x}, \boldsymbol{\xi})]$ in the worst-case distribution in normal days. In view of these facts, the planning model (16) inherits the advantages from both SP and RO: an exact PDF is not needed, and the optimal strategy is insensitive to the perturbation in the PDF of uncertain parameters. Indeed, due to the storage capabilities of ESU and TSU as well as the flexibility enabled by cogeneration and energy conversion, the system is also robust to the change of $\boldsymbol{\xi}$. This is simply a physical implication.

It should be pointed out that the worst-case distributions in the objective function (16a) for normal days and robust chance constraint (16c) for extreme days are not the same, and we can set up different ambiguity sets for (16a) and (16c). In these regards, we use P' and W' in reliability constraint (16c) to distinguish them from the ones appearing in the objective function (16a).

III. Solution Strategy

In formulation (16), the maximum expectation in (16a) and minimum probability evaluation over ambiguity set in (16c) prevent it from being solved directly. In this section, we derive tractable reformulations.

A. Reformulation of the Robust Chance Constraint

The robust chance constraint (16c) is difficult because it involves an infimum evaluation over an infinite set. It can be imaged that if (16c) is satisfied, then the probability evaluated under the reference distribution P_0 must be greater than $1-\alpha$, and the modifier must depend on the divergence measure and the confidence level. If the KL-divergence is used to measure the distance between PDFs, it is proven in [32] that constraint (16c) is equivalent to a traditional chance constraint

$$\Pr_0\{D_{loss} \le 0\} \ge 1 - \alpha_+ \tag{18}$$

where $\Pr_0$ indicates the probability evaluated under the reference distribution P_0; α_+ can be calculated by

$$\alpha_+ = \max\left\{0, 1 - \inf_{z \in (0,1)} \left\{ \frac{e^{-d_{KL}} z^{1-\alpha} - 1}{z - 1} \right\} \right\} \tag{19}$$

where the univariate function $h(z) = (e^{-d_{KL}} z^{1-\alpha} - 1)/(z - 1)$ is convex in z over the open interval $(0, 1)$ [32], so its minimum can be easily computed from the classical golden section search method or the first-order optimality condition that requires $\partial h(z)/\partial z = 0$. It is also revealed that $\alpha_+ < \alpha$, so (18) is more conservative than a traditional chance constraint evaluated at P_0.

This article has been accepted for publication in a future issue of this journal, but has not been fully edited. Content may change prior to final publication. Citation information: DOI 10.1109/TSTE.2018.2878230, IEEE Transactions on Sustainable Energy

However, chance constraint (18) is still non-convex [41]. A practical way is to find a conservative but convex approximation. It is obvious that (18) is equivalent to

$$E_{P_0}\left[\mathbb{I}_+(D_{loss})\right] = \Pr_0\{D_{loss} > 0\} \le \alpha_+ \tag{20}$$

where $E_{P_0}(\cdot)$ denotes expectation associated with the empirical distribution P_0; $\mathbb{I}_+(x)$ is an indicator function, i.e.,

$$\mathbb{I}_+(x) = \begin{cases} 1, & \text{if } x > 0 \\ 0, & \text{otherwise} \end{cases}$$

Now, we just need to find a convex function $\psi(x)$ that over estimates $\mathbb{I}_+(x)$ to ensure the approximation

$$E_{P_0}\left[\mathbb{I}_+(D_{loss})\right] \le E_{P_0}\left[\psi(D_{loss})\right] \le \alpha_+ \tag{21}$$

is conservative. If we require:

1) $\psi(x)$ is nondecreasing;

2) $\psi(0) = 1$.

It clearly over estimates $\mathbb{I}_+(x)$. In this paper, $\psi(D_{loss})$ is selected as follows

$$\psi(D_{loss}) = \max\{0, D_{loss}/\beta + 1\} \tag{22}$$

where $\beta > 0$ is a constant. Nevertheless, parameter β will be optimized in the final problem as such $\psi(D_{loss})$ provides a good approximation.

Perform SAA; suppose $\boldsymbol{\xi}^1, \boldsymbol{\xi}^2, \cdots, \boldsymbol{\xi}^K$ are typical scenarios with corresponding probabilities $\pi_1, \pi_2, \cdots, \pi_K$; then inequality $E_{P_0}\left[\psi(D_{loss})\right] \le \alpha_+$ renders

$$\sum_k \pi_k \max\{0, D_{loss}(\boldsymbol{\xi}^k)/\beta + 1\} \le \alpha_+$$

Multiplying both sides by β and introducing auxiliary variable ϕ_k, above inequality can be linearized as

$$\begin{aligned} &D_{loss}(\boldsymbol{\xi}^k) + \beta \le \phi_k,\ \phi_k \ge 0, \quad \forall k \\ &\sum_k \pi_k \phi_k \le \beta \alpha_+, \quad \beta > 0 \end{aligned} \tag{23}$$

The value of $D_{loss}(\boldsymbol{\xi}^k)$ is determined from problem (17). In the final problem, the minimization operator is no longer needed, and β is also a variable to be optimized. Details can be found in subsection C. Because we have employed α_+ which is more prudent than α, the reliability requirement in extreme days can be satisfied even if probabilities $\pi_1, \cdots, \pi_K$ are not entirely exact.

B. Reformulation of the Objective Function

For a given planning strategy $\boldsymbol{x}$, the worst-case expectation problem reads as follows:

$$\sup_{P \in W} E_P[Q(\boldsymbol{x}, \boldsymbol{\xi})] \tag{24}$$

Problem (24) entails optimizing a PDF, so it is an infinite-dimensional optimization problem. According to [42], the dual problem of (24) is the following univariate optimization problem

$$\min_{\lambda \ge 0}\ \lambda \log\left\{E_{P_0}\left[e^{Q(\boldsymbol{x},\boldsymbol{\xi})/\lambda}\right]\right\} + \lambda d_{KL} \tag{25}$$

where the decision variable is a non-negative scalar λ. For discrete distributions, the expectation in (25) can be replaced with a weighted-sum form

$$\min_{\lambda \ge 0}\ \lambda \log\left\{\sum_n \pi_n \left[e^{Q(\boldsymbol{x},\boldsymbol{\xi}^n)/\lambda}\right]\right\} + \lambda d_{KL} \tag{26}$$

Define $\theta_n = Q(\boldsymbol{x}, \boldsymbol{\xi}^n)$; In Appendix, we prove that

$$H(\theta, \lambda) = \lambda \log\left(\sum_n \pi_n e^{\theta_n/\lambda}\right) \tag{27}$$

is a convex function not only in λ but also in θ_n. Although θ_n is regarded as constant in the dual problem (26), however, it will be a decision variable in the final problem. Such convexity greatly facilitates algorithm development.

C. Final Problem and the Outer Approximation Algorithm

Based on aforementioned discussions, the energy hub planning problem (16) can be cast in the following form with a convex objective function and linear constraints.

$$\min \quad \boldsymbol{c}^T\boldsymbol{x} + \lambda \log\left(\sum_n \pi_n e^{\theta_n/\lambda}\right) + \lambda d_{KL} \tag{28a}$$

$$\text{s.t.} \quad \boldsymbol{x} \in X,\ \lambda \ge 0 \tag{28b}$$

$$\theta_n = \boldsymbol{p}^T\boldsymbol{y}^n,\ \forall n \tag{28c}$$

$$\boldsymbol{A}\boldsymbol{x} + \boldsymbol{B}\boldsymbol{y}^n + \boldsymbol{C}\boldsymbol{\xi}^n + \boldsymbol{d} \le 0,\ \forall n \tag{28d}$$

$$\boldsymbol{A'}\boldsymbol{x} + \boldsymbol{B'}\boldsymbol{y}^k + \boldsymbol{C'}\boldsymbol{\xi}^k + \boldsymbol{d'} \le 0,\ \forall k \tag{28e}$$

$$\boldsymbol{M}\boldsymbol{y}^k + \boldsymbol{N}\boldsymbol{\xi}^k \le g^k,\ \forall k \tag{28f}$$

$$g^k + \beta \le \phi_k,\ \phi_k \ge 0,\ \forall k \tag{28g}$$

$$\sum_{k=1}^K \pi_k \phi_k \le \beta \alpha_+,\ \beta > 0 \tag{28h}$$

In (28), scenarios in normal and extreme conditions are generated from three typical days and two extreme days, and independently labeled by n and k, respectively. The optimal second-stage cost $Q(\boldsymbol{x}, \boldsymbol{\xi}^n) = \boldsymbol{p}^T\boldsymbol{y}^n$ is denoted by θ_n in (28c); Load shedding is not allowed in normal conditions, as indicated by (28d); (28e)-(28f) quantify the minimum unserved nodal demands; (28g)-(28h) are reliability constraints for extreme conditions derived in (23), where the loss function $D_{loss}(\boldsymbol{\xi}^k) = g^k$.

Because the objective function (28a) is shown to be convex, and constraints (28b)-(28h) are polyhedral, any local algorithm or solver would converge, if succeeds, to the global optimum of (28). However, according to our preliminary test, general purpose nonlinear programming solvers, such as IPOPT and NLOPT, fail to converge when solving problem (28). To overcome this difficulty, an outer approximation (OA) algorithm is developed to solve (28) in an iterative manner. Basic procedures are summarized in Algorithm 1. This algorithm first linearizes the convex region defined by $H(\theta, \lambda) \le \sigma$, and successively generate cutting planes to approximate its boundary with increasingly high accuracy. As a result, only linear programs are solved. Finite convergence of OA algorithm for

This article has been accepted for publication in a future issue of this journal, but has not been fully edited. Content may change prior to final publication. Citation information: DOI 10.1109/TSTE.2018.2878230, IEEE Transactions on Sustainable Energy

Algorithm 1

1: Choose a convergence tolerance $\varepsilon > 0$; Set iteration index $m = 0$; Initialize θ^0 by solving SP model (10) and set $\lambda^0 = 1000$; calculate the value of $H^m = H(\theta^m, \lambda^m)$ as well as the gradient of $H(\theta, \lambda)$ at (θ^m, λ^m)

$$g_H^m = \left[\left(\frac{\partial H}{\partial \theta}\right)^T, \quad \frac{\partial H}{\partial \lambda}\right]\Big|_{(\theta^m, \lambda^m)}^T \tag{29}$$

2: Solve the following master LP

$$\begin{aligned} \min \quad & \boldsymbol{c}^T\boldsymbol{x} + \sigma + \lambda d_{KL} \\ \text{s.t.} \quad & (28b) - (28h) \\ & H^v + (g_H^v)^T \begin{bmatrix} \theta - \theta^v \\ \lambda - \lambda^v \end{bmatrix} \le \sigma, \\ & v = 0, 1, \cdots, m \end{aligned} \tag{30}$$

Update $m \leftarrow m + 1$, and record the optimal solution and the optimal value.

3: If the change of optimal values in two consecutive steps is less than ε, terminate and report the optimal solution as the final result; else calculate H^m and g_H^m according to (29), and add a new constraint

$$H^m + (g_H^m)^T \begin{bmatrix} \theta - \theta^m \\ \lambda - \lambda^m \end{bmatrix} \le \sigma \tag{31}$$

to the master LP (30) and go to step 2.

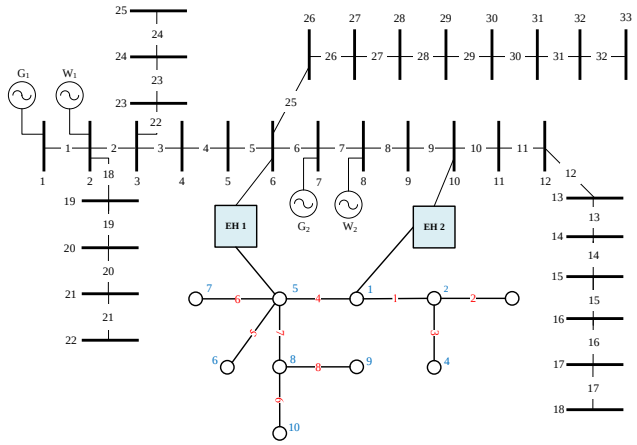

Fig. 2. Topology of integrated system.

TABLE I
COMPONENT DATA

	Parameters	Construction Cost
CHP	$\eta_{gp} = 0.9, \eta_{gh} = 0.9$	1000000 ($/MW)
HP	COP $= 3$	1500000 ($/MW)
ESU	$\eta_c^E = 0.98, \eta_d^E = 0.98, \mu^E = 0.01$	200000 ($/MWh)
TSU	$\eta_c^H = 0.95, \eta_d^H = 0.95, \mu^H = 0.01$	150000 ($/MWh)

convex programs has been established in [43]. According to our experiences, Algorithm 1 always converges in no more than 6 iterations for solving problem (28).

To compare the proposed DR-SP model with traditional SP and RO approaches, the supply reliability constraint in extreme days is augmented. For SP model (10), after performing convex approximation and SAA, the SP model is expressed as follows.

$$\begin{aligned} \min \ & \boldsymbol{c}^T\boldsymbol{x} + \sum_n \pi_n \boldsymbol{p}^T\boldsymbol{y}^n \\ \text{s.t.} \ & \boldsymbol{x} \in X, \ \boldsymbol{A}\boldsymbol{x} + \boldsymbol{B}\boldsymbol{y}^n + \boldsymbol{C}\boldsymbol{\xi}^n + \boldsymbol{d} \le 0, \ \forall n \\ & \boldsymbol{A'}\boldsymbol{x} + \boldsymbol{B'}\boldsymbol{y}^k + \boldsymbol{C'}\boldsymbol{\xi}^k + \boldsymbol{d'} \le 0, \ \forall k \\ & \boldsymbol{M}\boldsymbol{y}^k + \boldsymbol{N}\boldsymbol{\xi}^k \le g^k, \ \forall k \\ & g^k + \beta \le \phi_k, \ \phi_k \ge 0, \ \forall k \\ & \sum_{k=1}^K \pi_k \phi_k \le \beta\alpha, \ \beta > 0 \end{aligned} \tag{32}$$

RO model (11) could be amended as follows after adding supply reliability constraint.

$$\begin{aligned} \min_{\boldsymbol{x}} \ & \boldsymbol{c}^T\boldsymbol{x} + \max_{\boldsymbol{\xi}^n} \left\{ \min_{\boldsymbol{y}^n} \boldsymbol{p}^T\boldsymbol{y}^n \right\} \\ \text{s.t.} \ & \boldsymbol{x} \in X, \ \boldsymbol{A}\boldsymbol{x} + \boldsymbol{B}\boldsymbol{y}^n + \boldsymbol{C}\boldsymbol{\xi}^n + \boldsymbol{d} \le 0, \ \forall n \\ & \boldsymbol{A'}\boldsymbol{x} + \boldsymbol{B'}\boldsymbol{y}^k + \boldsymbol{C'}\boldsymbol{\xi}^k + \boldsymbol{d'} \le 0, \ \forall k \\ & \boldsymbol{M}\boldsymbol{y}^k + \boldsymbol{N}\boldsymbol{\xi}^k \le 0, \ \forall k \end{aligned} \tag{33}$$

In (33), load shedding is not allowed even in extreme days, which is in line with the basic paradigm of RO. Unlike a traditional RO model which uses an uncertainty set, (33) copes with a finite number of scenarios. Nonetheless, it is equivalent to considering the convex hull of $\{\boldsymbol{\xi^n}\}$ as the uncertainty set.

IV. CASE STUDIES

A test system comprised of a modified IEEE 33-bus PDN and a 10-node DHN is used to validate the performance of the proposed model and algorithm. System topology is shown in Fig. 2 and system data are available in [44]. Two energy hubs are to be invested within the period of ten years. Energy hub component data are listed in Table I. All experiments are conducted on a laptop with Intel i5-7300HQ CPU and 8G memory. All optimization models are established by YALMIP in MATLAB. LP is solved by CPLEX12.8.

For the uncertain factors, electric/thermal demands and wind generation profiles in three typical days (spring/autumn, summer, and winter) are employed in normal condition constraint (28d); two extremal days in summer and winter are particularly treated in (28e)-(28f). The predicted data are plotted in Fig. 3. We assume that the forecast error obey Normal distribution with zero mean, and the standard deviation is 0.2 times of forecast values for wind power, and 0.1 times of forecast values for system load. To perform SAA, 5000 scenarios are generated for each representative day. Based on the back-forward scenario reduction method [45], 100 scenarios are selected for normal and extreme days. According to (15), $d_{KL} = 0.0124$ is used in (12) with confidence level $\alpha^* = 0.95$; In the robust chance constraint (16c), the reliability level is maintained no less than 95%, which means $\alpha = 0.05$ and $\alpha_+ = 0.0229$, in light of (19).

This article has been accepted for publication in a future issue of this journal, but has not been fully edited. Content may change prior to final publication. Citation information: DOI 10.1109/TSTE.2018.2878230, IEEE Transactions on Sustainable Energy

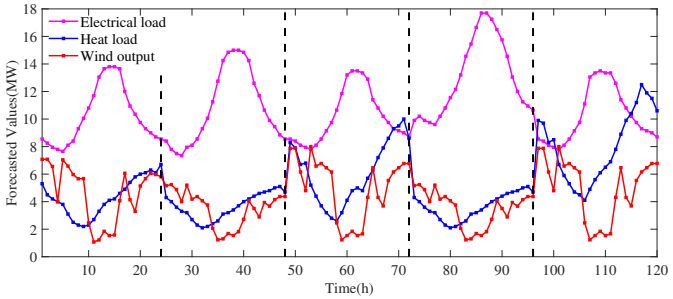

Fig. 3. Electrical loads, heat loads and wind power outputs in different cases. (from left to right: three typical days in spring/autumn, summer and winter; two extreme days in summer and winter)

TABLE II
OPTIMAL INVESTMENT STRATEGIES

		DR-SP	SP	RO
EH_1	CHP (MW)	5.8732	5.6406	6.1008
	HP (MW)	2.6416	2.6325	2.5780
	ESU (MWh)	3.8214	4.0569	4.0688
	TSU (MWh)	6.8870	6.7553	6.6172
EH_2	CHP (MW)	5.9455	5.7004	6.1711
	HP (MW)	2.6013	2.5917	2.5393
	ESU (MWh)	3.8665	4.0572	4.0786
	TSU (MWh)	6.8611	6.7520	6.5141
Optimum (10^7\$)		8.0282	7.9391	8.6954
Investment Cost (10^7\$)		2.3283	2.2826	2.3547
Operation Cost (10^7\$)		5.6999	5.6565	6.3407
Computation Time(s)		847	128	91

The proposed DR-SP model (28) is compared with traditional SP model (32) and RO model (33). The planning results offered by the three approaches are compared in Table II. Clearly, in terms of the optimal value, DR-SP is more (less) conservative than the traditional SP (RO), because SP only accounts for the reference distribution P_0, and RO neglects the dispersion effect of uncertain parameters. It is also observed that the RO model prefers to invest on CHP units as it is the most flexible component, and results in the highest cost. Compared to SP, system flexibility in normal conditions and reliability under extreme conditions can be guaranteed by deploying the planning strategy offered by DR-SP, at the cost of 1.12% additional expenditure. The computation time of three models is also shown in Table II. Algorithm 1 for DR-SP model takes 847s to converge within 6 iterations, which is acceptable in a planning problem.

Parameter d_{KL} interprets the decision-maker's confidence on the accuracy of empirical distribution. The larger d_{KL}, the better the system is protected against distributional uncertainty. In this set of tests, we investigate the impact of data availability and confidence level α^* in W. These two factors lead to different values of d_{KL}, according to (15). Results are exhibited in Table III. The optimal values increase moderately with the growth of d_{KL}; even if only 100 samples are used for setting up the ambiguity set, the overall cost is still smaller than that in RO. We also observe that data availability has larger impact on

TABLE III
OPTIMUMS WITH DIFFERENT VALUES OF d_{KL}

d_{KL} & Optimum(10^7\$) \ α^* / M	0.90	0.95	0.99
5000	0.0118 & 8.0261	0.0124 & 8.0282	0.0136 & 8.0322
2000	0.0296 & 8.0800	0.0311 & 8.0844	0.0340 & 8.0930
1000	0.0592 & 8.1211	0.0622 & 8.1234	0.0679 & 8.1278
500	0.1185 & 8.1597	0.1243 & 8.1629	0.1358 & 8.1690
100	0.5925 & 8.3167	0.6217 & 8.3231	0.6790 & 8.3381

TABLE IV
FAILURE EVENTS WITH DIFFERENT KL DIVERGENCE DISTANCE

d_p^0		0.005	0.010	0.020	0.030	0.050
DR-SP	$\Pr_1$	2.36%	2.92%	3.74%	4.41%	5.52%
	$\Pr_2$	2.22%	2.75%	3.55%	4.19%	5.27%
SP	$\Pr_1$	4.26%	5.02%	6.15%	7.06%	8.57%
	$\Pr_2$	4.13%	4.88%	5.99%	6.89%	8.37%

the total cost than parameter α^*. In all these tests, Algorithm 1 successfully converges in 6 iterations and the computation time is less than 900s, demonstrating the efficiency of the proposed method in a planning problem with a long time horizon.

A main advantage of the DR-SP model is that its optimal solution is insensitive to PDF perturbations. In this experiment, we generate data sets consisting of 10000 scenarios whose distribution is different from the reference one. Their KL divergence distance d_p^0 is calculated from (14). We test the probability of demand loss events under each data set. Results are provided in Table IV, where $\Pr_1$ / $\Pr_2$ denotes the failure probability in the extreme summer/winter day. Under the planning strategies offered by the traditional SP model, the failure probabilities in extreme days exceed the designated value once $d_p^0 > 0.01$. Under the planning strategies offered by the DR-SP model, when $d_p^0 < 0.0124$, the value used in W, the reliability level is greater than 97% even if the real data follows a different distribution, demonstrating the distributional robustness of planning strategies. In fact, the reliability level can be maintained even d_p^0 grows to 0.03. This is because we use convex function $\psi(x)$ to approximate the indicator function $\mathbb{I}_+(x)$, resulting in the conservative inequality (21). Further increase of d_p^0 wrecks the reliability requirement, as shown in the last column of Table IV.

Energy storage units play a central role in the daily operation of energy hub. In the future, the unit capacity costs of both ESU and TSU are expected to drop continuously. In this experiment, we change the investment cost coefficients of storage units by multiplying their values in Table I with a scalar ζ. Results are given in Table V. We can see that storage capacity increase rapidly with the deceasing of investment cost. Meanwhile, CHP unit capacity decreases significantly while heat pump capacity grows slightly due to the growing size of TSU. These results indicate that the need for energy storage may witness fast growth in future integrated systems.

Finally, we investigate the impact of wind penetration level.

This article has been accepted for publication in a future issue of this journal, but has not been fully edited. Content may change prior to final publication. Citation information: DOI 10.1109/TSTE.2018.2878230, IEEE Transactions on Sustainable Energy

TABLE V
INVESTMENT STRATEGIES WITH DIFFERENT STORAGE COSTS

	ζ	1.0	0.8	0.6	0.4
EH_1	CHP (MW)	5.8732	5.3492	3.3455	3.0995
	HP (MW)	2.6416	2.7203	2.9550	3.0594
	ESU (MWh)	3.8214	5.8367	14.6498	15.7582
	TSU (MWh)	6.8870	8.1579	13.4595	14.2451
EH_2	CHP (MW)	5.9455	5.4157	3.3896	3.1393
	HP (MW)	2.6013	2.6767	2.9060	3.0067
	ESU (MWh)	3.8665	5.8203	14.5244	15.6491
	TSU (MWh)	6.8611	8.1389	13.4434	14.2272
Optimum (10^7\$)		8.0282	7.9438	7.7950	7.5944
Investment Cost (10^7\$)		2.3283	2.3636	2.5397	2.5890
Operation Cost (10^7\$)		5.6999	5.5802	5.2553	5.0054

TABLE VI
RESULTS WITH DIFFERENT WIND PENETRATION LEVELS

Wind Capacity		6MW	8MW	10MW	12MW
EH_1	CHP (MW)	6.4103	5.8732	4.9633	3.6916
	HP (MW)	2.5695	2.6416	2.8034	2.9743
	ESU (MWh)	3.0106	3.8214	6.2506	10.7163
	TSU (MWh)	5.5171	6.8870	8.9294	12.1764
EH_2	CHP (MW)	6.4923	5.9455	5.0227	3.7299
	HP (MW)	2.5327	2.6013	2.7678	2.9206
	ESU (MWh)	3.0770	3.8665	6.2979	10.6220
	TSU (MWh)	5.5207	6.8611	8.9499	12.1630
Optimum (10^7\$)		8.8974	8.0282	7.2216	6.4713
Investment Cost (10^7\$)		2.3429	2.3283	2.3534	2.4182
Operation Cost (10^7\$)		6.5545	5.6999	4.8682	4.0531

In this test, the wind farm output given in Fig. 2 is multiplied by a constant. Its capacity refers to the maximum output throughout the day. Results are shown in Table VI. We can see when more wind energy is available to use, the excessive electricity produced during night can be stored in ESU or converted into heat and stored in TSU, so the capacity of storage units grows significantly. Meanwhile, larger heat pump is built to produce thermal energy from electric power, which is used to supply peak heat demand and charge the TSU. Consequently, the capacity of CHP unit decreases because more energy will be produced by wind turbines with zero operation cost, while dispatching CHP unit incurs non-zero gas fuel cost.

V. CONCLUSION

This paper proposes a data-driven robust stochastic programming model for determining capacities of components in an energy hub in multi-carrier energy networks. The proposed method shows two appealing features: first, it makes no reference to the exact distributions of uncertain factors while accounts for the dispersion effect; second, it remains computationally tractable because of the convex nature and the linear programming based algorithm. The proposed model properly considers operating constraints and reliability requirements in the planning stage, and thus could offer more informative reference to the decision maker.

Case studies deliver the following implications: From the methodology point of view, the model conservatism is acceptable for planning oriented applications; the reliability is robust against the perturbation in renewable generation and load probability distributions, which is called distributional robustness. In short, the proposed model offers more robust and less conservative planning strategies compared to existing approaches, and its conservatism is adjustable for decision makers. From the investment tendency point of view, with the continuous drop of storage construction cost and the increasing penetration level of renewables, the need for energy storage in the integrated energy system will grow rapidly.

APPENDIX

Proposition 1: Function

$$H(\theta, \lambda) = \lambda \log \left(\sum_n \pi_n e^{\theta_n / \lambda} \right)$$

is convex in both of its inputs θ and λ.

Proof: First, we claim that the following function is convex (page 87, in Example 3.14, [46])

$$h_1(\theta) = \log \left(\sum_{n=1}^{N} \mathrm{e}^{\theta_n} \right)$$

Second, because the composition with an affine mapping preserves convexity (Sect. 3.2.2, [46]), a new function

$$h_2(\theta) = h_1(A\theta + b)$$

remains convex under linear mapping $\theta \to A\theta + b$. Let A be an identity matrix, and

$$b = [\log \pi_1, \cdots, \log \pi_N]^T$$

then we have

$$h_2(\theta) = \log \left(\sum_{n=1}^{N} \pi_n \mathrm{e}^{\theta_n} \right)$$

is a convex function; At last, function

$$H(\theta, \lambda) = \lambda h_2(\theta / \lambda)$$

is the perspective of convex function $h_2(\theta)$, so is convex in both inputs θ and λ (Sect. 3.2.6, [46]).

REFERENCES

[1] S. Heinen, C. Hewicker, N. Jenkins, J. McCalley, M. O'Malley, S. Pasini, and S. Simoncini, "Unleashing the flexibility of gas: Innovating gas systems to meet the electricity system's flexibility requirements," *IEEE Power Energy Mag.*, vol. 15, no. 1, pp. 16–24, Jan. 2017.

[2] N. Good and P. Mancarella, "Flexibility in multi-energy communities with electrical and thermal storage: A stochastic, robust approach for multi-service demand response," *IEEE Trans. Smart Grid*, Sep. 2017.

[3] S. Li, J. Sui, H. Jin, and J. Zheng, "Full chain energy performance for a combined cooling, heating and power system running with methanol and solar energy," *Appl. Energy*, vol. 112, pp. 673–681, Dec. 2013.

[4] J. Fang, Q. Zeng, X. Ai, Z. Chen, and J. Wen, "Dynamic optimal energy flow in the integrated natural gas and electrical power systems," *IEEE Trans. Sustain. Energy*, vol. 9, no. 1, pp. 188–198, Jan. 2018.

[5] T. Krause, G. Andersson, K. Frohlich, and A. Vaccaro, "Multiple-energy carriers: modeling of production, delivery, and consumption," *Proc. IEEE*, vol. 99, no. 1, pp. 15–27, Jan. 2011.

[6] F. Kienzle, P. Ahcin, and G. Andersson, "Valuing investments in multi-energy conversion, storage, and demand-side management systems under uncertainty," *IEEE Trans. Sustain. Energy*, vol. 2, no. 2, pp. 194–202, Apr. 2011.

[7] M. Geidl and G. Andersson, "Optimal power flow of multiple energy carriers," *IEEE Trans. Power Syst.*, vol. 22, no. 1, pp. 145–155, Feb. 2007.

[8] M. Geidl, G. Koeppel, P. Favre-Perrod, B. Klockl, G. Andersson, and K. Frohlich, "Energy hubs for the future," *IEEE Power Energy Mag.*, vol. 5, no. 1, pp. 24–30, Jan. 2007.

[9] M. C. Bozchalui, S. A. Hashmi, H. Hassen, C. A. Cañizares, and K. Bhattacharya, "Optimal operation of residential energy hubs in smart grids," *IEEE Trans. Smart Grid*, vol. 3, no. 4, pp. 1755–1766, Dec. 2012.

[10] A. Dolatabadi, M. Jadidbonab, and B. Mohammadi-Ivatloo, "Short-term scheduling strategy for wind-based energy hub: A hybrid stochastic/IGDT approach," *IEEE Trans. Sustain. Energy*, vol. PP, no. 99, pp. 1–1, Jan. 2018.

[11] I. G. Moghaddam, M. Saniei, and E. Mashhour, "A comprehensive model for self-scheduling an energy hub to supply cooling, heating and electrical demands of a building," *Energy*, vol. 94, pp. 157–170, Jan. 2016.

[12] M. Rastegar and M. Fotuhi-Firuzabad, "Load management in a residential energy hub with renewable distributed energy resources," *Energy Build.*, vol. 107, pp. 234–242, Nov. 2015.

[13] M. Moeini-Aghtaie, A. Abbaspour, M. Fotuhi-Firuzabad, and E. Hajipour, "A decomposed solution to multiple-energy carriers optimal power flow," *IEEE Trans. Power Syst.*, vol. 29, no. 2, pp. 707–716, Mar. 2014.

[14] C. Shao, X. Wang, M. Shahidehpour, X. Wang, and B. Wang, "An MILP-based optimal power flow in multicarrier energy systems," *IEEE Trans. Sustain. Energy*, vol. 8, no. 1, pp. 239–248, Jan. 2017.

[15] H. R. Massrur, T. Niknam, J. Aghaei, M. Shafie-Khah, and J. P. S. Catalao, "Fast decomposed energy flow in large-scale integrated electricity-gas-heat energy systems," *IEEE Trans. Sustain. Energy*, vol. PP, no. 99, pp. 1–1, Jan. 2018.

[16] Y. Wang, N. Zhang, Z. Zhuo, C. Kang, and D. Kirschen, "Mixed-integer linear programming-based optimal configuration planning for energy hub: Starting from scratch," *Appl. Energy*, vol. 210, pp. 1141–1150, Jan. 2018.

[17] W. Huang, N. Zhang, J. Yang, Y. Wang, and C. Kang, "Optimal configuration planning of multi-energy systems considering distributed renewable energy," *IEEE Trans. Smart Grid*, Oct. 2017.

[18] X. Zhang, M. Shahidehpour, A. Alabdulwahab, and A. Abusorrah, "Optimal expansion planning of energy hub with multiple energy infrastructures," *IEEE Trans. Smart Grid*, vol. 6, no. 5, pp. 2302–2311, Sep. 2015.

[19] M. Salimi, H. Ghasemi, M. Adelpour, and S. Vaez-ZAdeh, "Optimal planning of energy hubs in interconnected energy systems: a case study for natural gas and electricity," *IET Gener. Transm. Dis.*, vol. 9, no. 8, pp. 695–707, May 2015.

[20] X. Zhang, C. Liang, M. Shahidehpour, A. Alabdulwahab, and A. Abusorrah, "Reliability-based optimal planning of electricity and natural gas interconnections for multiple energy hubs," *IEEE Trans. Smart Grid*, vol. 8, no. 4, pp. 1658–1667, Jul. 2017.

[21] S. Pazouki and M.-R. Haghifam, "Optimal planning and scheduling of energy hub in presence of wind, storage and demand response under uncertainty," *Int. J. Elect. Power Energy Syst.*, vol. 80, pp. 219–239, Sep. 2016.

[22] A. Dolatabadi, B. Mohammadi-ivatloo, M. Abapour, and S. Tohidi, "Optimal stochastic design of wind integrated energy hub," *IEEE Trans. Ind. Inform.*, vol. 13, no. 5, pp. 2379–2388, Oct. 2017.

[23] N. Neyestani, M. Yazdani-Damavandi, M. Shafie-Khah, G. Chicco, and J. P. Catalão, "Stochastic modeling of multienergy carriers dependencies in smart local networks with distributed energy resources," *IEEE Trans. Smart Grid*, vol. 6, no. 4, pp. 1748–1762, Jul. 2015.

[24] S. Hemmati, S. F. Ghaderi, and M. S. Ghazizadeh, "Sustainable energy hub design under uncertainty using benders decomposition method," *Energy*, vol. 143, pp. 1029–1047, Jan. 2018.

[25] A. Parisio, C. Del Vecchio, and A. Vaccaro, "A robust optimization approach to energy hub management," *Int. J. Elect. Power Energy Syst.*, vol. 42, no. 1, pp. 98–104, Nov. 2012.

[26] C. He, L. Wu, T. Liu, and Z. Bie, "Robust co-optimization planning of interdependent electricity and natural gas systems with a joint N-1 and probabilistic reliability criterion," *IEEE Trans. Power Syst.*, vol. 33, no. 2, pp. 2140–2154, Mar. 2018.

[27] Z. Li, W. Wu, J. Wang, B. Zhang, and T. Zheng, "Transmission-constrained unit commitment considering combined electricity and district heating networks." *IEEE Trans. Sustain. Energy*, vol. 7, no. 2, pp. 480–492, Apr. 2016.

[28] M. Zugno, J. M. Morales, and H. Madsen, "Commitment and dispatch of heat and power units via affinely adjustable robust optimization," *Comput. Oper. Res.*, vol. 75, pp. 191–201, Nov. 2016.

[29] D. Bertsimas and A. Thiele, "A robust optimization approach to inventory theory," *Oper. Res.*, vol. 54, no. 1, pp. 150–168, Feb. 2006.

[30] E. Delage and Y. Ye, "Distributionally robust optimization under moment uncertainty with application to data-driven problems," *Oper. Res.*, vol. 58, no. 3, pp. 595–612, Jun. 2010.

[31] W. Wiesemann, D. Kuhn, and M. Sim, "Distributionally robust convex optimization," *Oper. Res.*, vol. 62, no. 6, pp. 1358–1376, Oct. 2014.

[32] R. Jiang and Y. Guan, "Data-driven chance constrained stochastic program," *Math. Program.*, vol. 158, no. 1-2, pp. 291–327, Jan. 2016.

[33] Z. Li, Q. Guo, H. Sun, and J. Wang, "Sufficient conditions for exact relaxation of complementarity constraints for storage-concerned economic dispatch," *IEEE Trans. Power Syst.*, vol. 31, no. 2, pp. 1653–1654, Mar. 2016.

[34] M. E. Baran and F. F. Wu, "Network reconfiguration in distribution systems for loss reduction and load balancing," *IEEE Trans. Power Del.*, vol. 4, no. 2, pp. 1401–1407, Apr. 1989.

[35] X. Liu, J. Wu, N. Jenkins, and A. Bagdanavicius, "Combined analysis of electricity and heat networks," *Appl. Energy*, vol. 162, pp. 1238–1250, Jan. 2016.

[36] C. Wang, W. Wei, J. Wang, L. Wu, and Y. Liang, "Equilibrium of interdependent gas and electricity markets with marginal price based bilateral energy trading," *IEEE Trans. Power Syst.*, Jan. 2018.

[37] L. Wu, "A tighter piecewise linear approximation of quadratic cost curves for unit commitment problems," *IEEE Trans. Power Syst.*, vol. 26, no. 4, p. 2581, Nov. 2583.

[38] J. Rice, *Mathematical statistics and data analysis*. Nelson Education, 2006.

[39] S. Kullback, *Information theory and statistics*. Courier Corporation, 1997.

[40] L. Pardo, *Statistical inference based on divergence measures*. CRC press, 2005.

[41] A. Nemirovski and A. Shapiro, "Convex approximations of chance constrained programs," *SIAM J. Optimiz.*, vol. 17, no. 4, pp. 969–996, Nov. 2006.

[42] Z. Hu and L. J. Hong, "Kullback-leibler divergence constrained distributionally robust optimization," *Optimization Online*, 2013.

[43] W. W. Hogan, "Applications of a general convergence theory for outer approximation algorithms," *Math. program.*, vol. 5, no. 1, pp. 151–168, Dec. 1973.

[44] https://sites.google.com/163.com/caoyang13.

[45] J. Dupačová, N. Gröwe-Kuska, and W. Römisch, "Scenario reduction in stochastic programming," *Math. program.*, vol. 95, no. 3, pp. 493–511, Mar. 2003.

[46] S. Boyd and L. Vandenberghe, *Convex optimization*. Cambridge University Press, 2004.

Yang Cao (S'18) received the B.Sc. degree in electrical engineering from Tsinghua University, Beijing, China, in 2017, where he is currently pursuing the Ph.D. degree.

His research interests include planning and operation of multi-carrier energy systems.

This article has been accepted for publication in a future issue of this journal, but has not been fully edited. Content may change prior to final publication. Citation information: DOI 10.1109/TSTE.2018.2878230, IEEE Transactions on Sustainable Energy

Wei Wei (M'15-SM'18) received the Bachelor and Ph.D. degrees both in electrical engineering from Tsinghua University, Beijing, China, in 2008 and 2013, respectively.

He was a Postdoctoral Researcher with Tsinghua University from 2013 to 2015. He was a Visiting Scholar with Cornell University, Ithaca, NY, USA, in 2014, and with Harvard University, Cambridge, MA, USA, in 2015. He is currently an Assistant Professor with Tsinghua University. His research interests include applied optimization and energy system economics.

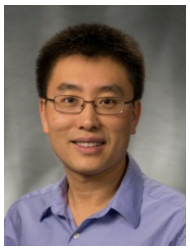

Jianhui Wang (M'07-SM'12) received the Ph.D. degree in electrical engineering from Illinois Institute of Technology, Chicago, IL, USA, in 2007.

Presently, he is an Associate Professor with the Department of Electrical Engineering at Southern Methodist University, Dallas, Texas, USA. Prior to joining SMU, Dr. Wang had an eleven-year stint at Argonne National Laboratory with the last appointment as Section Lead - Advanced Grid Modeling.

Dr. Wang is the secretary of the IEEE Power and Energy Society (PES) Power System Operations, Planning and Economics Committee. He has held visiting positions in Europe, Australia and Hong Kong including a VELUX Visiting Professorship at the Technical University of Denmark (DTU). Dr. Wang is the Editor-in-Chief of the IEEE Transactions on Smart Grid and an IEEE PES Distinguished Lecturer. He is also the recipient of the IEEE PES Power System Operation Committee Prize Paper Award in 2015.

Shengwei Mei (F'15) received the B.Sc. degree in mathematics from Xinjiang University, Urumqi, China, the M.Sc. degree in operations research from Tsinghua University, Beijing, China, and the Ph.D. degree in automatic control from Chinese Academy of Sciences, Beijing, China, in 1984, 1989, and 1996, respectively.

He is currently a Professor of Tsinghua University, Beijing, China. His research interests include power system complexity and control, game theory and its application in power systems.

Miadreza Shafie-khah (M'13-SM'17) received the M.Sc. and Ph.D. degrees in electrical engineering from Tarbiat Modares University, Tehran, Iran, in 2008 and 2012, respectively. He received his first postdoc from the University of Beira Interior (UBI), Covilha, Portugal in 2015, while working on the 5.2-million-euro FP7 project SiNGULAR ("Smart and Sustainable Insular Electricity Grids Under Large-Scale Renewable Integration"). He received his second postdoc from the University of Salerno, Salerno, Italy in 2016.

He was considered one of the Outstanding Reviewers of the IEEE TRANSACTIONS ON SUSTAINABLE ENERGY, in 2014 and 2017, one of the Best Reviewers of the IEEE TRANSACTIONS ON SMART GRID, in 2016 and 2017, and one of the Outstanding Reviewers of the IEEE TRANSACTIONS ON POWER SYSTEMS, in 2017. His research interests include power market simulation, market power monitoring, power system optimization, demand response, electric vehicles, price forecasting and smart grids.

João P. S. Catalão (M'04-SM'12) received the M.Sc. degree from the Instituto Superior Técnico (IST), Lisbon, Portugal, in 2003, and the Ph.D. degree and Habilitation for Full Professor ("Agregação") from the University of Beira Interior (UBI), Covilha, Portugal, in 2007 and 2013, respectively.

Currently, he is a Professor at the Faculty of Engineering of the University of Porto (FEUP), Porto, Portugal, and Researcher at INESC TEC, INESC-ID/IST-UL, and C-MAST/UBI. He was also appointed as Visiting Professor by North China Electric Power University, Beijing, China. He was the Primary Coordinator of the EU-funded FP7 project SiNGULAR ("Smart and Sustainable Insular Electricity Grids Under Large-Scale Renewable Integration"), a 5.2-million-euro project involving 11 industry partners. He has authored or coauthored more than 675 publications, including 252 journal papers (more than 75 IEEE Transactions/Journal papers), 370 conference proceedings papers, 5 books, 34 book chapters, and 14 technical reports, with an h-index of 43, an i10-index of 173, and over 7380 citations (according to Google Scholar), having supervised more than 70 post-docs, Ph.D. and M.Sc. students. He is the Editor of the books entitled *"Electric Power Systems: Advanced Forecasting Techniques and Optimal Generation Scheduling and Smart and Sustainable Power Systems: Operations, Planning and Economics of Insular Electricity Grids"* (Boca Raton, FL, USA: CRC Press, 2012 and 2015, respectively). His research interests include power system operations and planning, hydro and thermal scheduling, wind and price forecasting, distributed renewable generation, demand response and smart grids.

Prof. Catalão is an Editor of the IEEE TRANSACTIONS ON SMART GRID, an Editor of the IEEE TRANSACTIONS ON POWER SYSTEMS, an Associate Editor of the IEEE TRANSACTIONS ON INDUSTRIAL INFORMATICS, and a Subject Editor of the *IET Renewable Power Generation*. From 2011 till 2018 (seven years) he was an Editor of the IEEE TRANSACTIONS ON SUSTAINABLE ENERGY and an Associate Editor of the *IET Renewable Power Generation*. He was the Guest Editor-in-Chief for the Special Section on "Real-Time Demand Response" of the IEEE TRANSACTIONS ON SMART GRID, published in December 2012, the Guest Editor-in-Chief for the Special Section on "Reserve and Flexibility for Handling Variability and Uncertainty of Renewable Generation" of the IEEE TRANSACTIONS ON SUSTAINABLE ENERGY, published in April 2016, and the Corresponding Guest Editor for the Special Section on "Industrial and Commercial Demand Response" of the IEEE TRANSACTIONS ON INDUSTRIAL INFORMATICS, to be published in November 2018. Since March 2018, he is the Lead Guest Editor for the Special Issue on "Demand Side Management and Market Design for Renewable Energy Support and Integration" of the *IET Renewable Power Generation*. He was the recipient of the 2011 Scientific Merit Award UBI-FE/Santander Universities, the 2012 Scientific Award UTL/Santander Totta, the 2016 FEUP Diploma of Scientific Recognition, and the Best INESC-ID Researcher 2017 Award, in addition to an Honorable Mention in the 2017 Scientific Awards ULisboa/Santander Universities. Moreover, he has won 4 Best Paper Awards at IEEE Conferences.